Journal of Alloys and Compounds 509 (2011) 3852–3854

Contents lists available at ScienceDirect

Journal of Alloys and Compounds

journal homepage: www.elsevier.com/locate/jallcom

Vacuum ultraviolet spectroscopic properties of $KSrPO_4:Tb^{3+}$

Feng Zhang, Yuhua Wang*, Jidi Liu

Department of Materials Science, Lanzhou University, Lanzhou 730000, PR China

ARTICLE INFO

Article history:
Received 3 November 2009
Accepted 16 December 2010
Available online 24 December 2010

Keywords:
$KSrPO_4:Tb^{3+}$
VUV
Photoluminescence properties

ABSTRACT

$KSrPO_4:Tb^{3+}$ phosphors were prepared by a solid-state method and their photoluminescence properties were investigated under vacuum ultraviolet excitation. In the excitation spectrum monitoring at 544 nm, the band in the region of 120–162 nm can be attributed to be the overlap of host absorption and charge transfer transition of $O^{2-} \rightarrow Tb^{3+}$, and the band ranging from 162 to 300 nm was assigned to the f–d transition of Tb^{3+}. The photoluminescence spectrum shows that the phosphors exhibited a strong green emission around 544 nm corresponding to the $^5D_4 \rightarrow {}^7F_5$ transition of Tb^{3+} under the excitation of 147 nm. Optimal emission intensity was obtained when $x = 7\%$ in $KSr_{1-x}PO_4:xTb^{3+}$ and the luminescent chromaticity coordinates were calculated to be ($x = 0.317$, $y = 0.522$) for $KSr_{0.93}PO_4:7\%Tb^{3+}$.

1. Introduction

Recently, the photoluminescence properties of rare earth ions in different hosts in the vacuum ultraviolet (VUV) range have attracted much attention due to practical application such as plasma display phosphors (PDPs), mercury-free lamps and liquid crystal displays (LCDs) backlights [1–4]. Plasma resonance VUV radiation lines at 147 or 172 nm from Xe/He gas plasma are used for the phosphor excitation to emit visible luminescence [5–7]. Thus, the design of phosphor should consider that the phosphor host itself or doped activators can absorb around these wavelengths efficiently. In addition, phosphors for commercial purpose are required to have high conversion efficiency under VUV excitation, good colorimetric purity, and proper decay time [8–10]. As for the green component $Zn_2SiO_4:Mn^{2+}$ which is widely used in PDP due to its good color purity and high luminous brightness, however, it has a long decay time resulting in a serious lag in image transformation due to the parity-and spin-forbidden $^4T_1 \rightarrow {}^6A_1$ transition of Mn^{2+} [4]. It is urgent to explore novel green phosphors with shorter decay time and high luminescent efficiency. Some complex oxides, such as borates, silicates, aluminates and phosphates having strong absorption in the VUV range were widely investigated [11–15].

Recently, $KSrPO_4$ has drawn increasing attention due to their excellent thermal stability, chemical stability and hydrolytic stability, which can provide opportunities for developing efficient VUV phosphors. $KSrPO_4$ has been reported to have a ß-K_2SO_4 structure with space group of *Pnma* [16]. The structure is formed by regular PO_4^{3-} tetrahedral surrounding the monovalent cation K^+ and divalent cation Sr^{2+} in tenfold and ninefold coordinations, respectively. The large-size divalent cation Sr^{2+} (1.12 Å) can be substituted by RE (RE = Eu^{2+}, Sm^{3+}, Tb^{3+}) to achieve full-color luminescence [17]. Up to now, much previous work focused mainly on the luminescence properties in the ultraviolet (UV) region [17–19] and little attention has been paid to the VUV optical properties. In this study, the new green-emitting VUV phosphor $KSrPO_4:Tb^{3+}$ was prepared and the photoluminescence (PL) properties were investigated.

2. Experimental

The compounds $KSr_{1-x}PO_4:xTb^{3+}$ ($1\% \le x \le 11\%$), $KSrPO_4:0.5\%Eu^{2+}$, $KSrPO_4:2\%Eu^{3+}$ were prepared via a solid-state reaction by adopting K_2CO_3 (99%), $Sr(NO_3)_2$ (99.5%), $(NH_4)_2HPO_4$(98.5%), Tb_4O_7 (99.99%) and Eu_2O_3 (99.99%) as starting materials. Stoichiometric amounts of the starting materials were mixed together on an agate mortar by using ethanol. The mixtures were prefired at 500 °C for 4 h in air and then fired at 1200 °C for 6 h under 5% H_2/N_2 mixed-gas atmosphere for preparing $KSr_{1-x}PO_4:xTb^{3+}$ ($1\% \le x \le 11\%$) and $KSrPO_4:0.5\%Eu^{2+}$ samples. $KSrPO_4:Eu^{3+}$ were prepared at 500 °C for 4 h and then hold at 1200 °C for 6 h in air. The final products were obtained by cooling down to room temperature in the furnace.

The phase purity of all the samples was characterized and evaluated by using Rigaku D/max-2400 X-ray diffractometer with Ni-filtered Cu $K\alpha$ ($\lambda = 1.54178$ Å) radiation operated at 40 kV and 60 mA. The 2θ ranges of all the data sets are from 10° to 80° with the step size of 0.02°. The VUV excitation and emission spectra were measured by an FLS-920T fluorescence spectrophotometer with a VM-504 VUV monochromator using a deuterium lamp as the lighting source. The excitation spectra were corrected with sodium salicylate powder. All measurements were operated at room temperature.

3. Results and discussion

The X-ray diffraction (XRD) patterns of as-prepared samples and the standard pattern were shown and compared in Fig. 1. A careful analysis of the patterns shows that $KSr_{0.995}PO_4:0.5\%Eu^{2+}$,

* Corresponding author at: Department of Material Science, School of Physical Science and Technology, Lanzhou University, Lanzhou 730000, PR China.
Tel.: +86 931 8912772; fax: +86 931 8913554; mobile: +86 13919816967.
E-mail address: wyh@lzu.edu.cn (Y. Wang).

0925-8388/$ – see front matter © 2011 Elsevier B.V. All rights reserved.
doi:10.1016/j.jallcom.2010.12.123

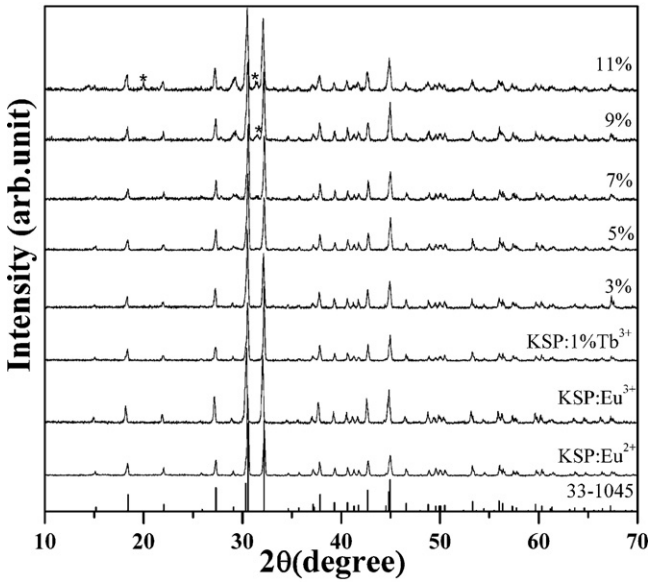

Fig. 1. X-ray diffraction (XRD) patterns of $KSr_{0.995}PO_4$:0.5%Eu^{2+}, $KSr_{0.98}PO_4$:2%Eu^{3+} and $KSr_{1-x}PO_4$:xTb^{3+} ($1\% \le x \le 11\%$) samples.

$KSr_{0.98}PO_4$:2%Eu^{3+} and $KSr_{1-x}PO_4$:xTb^{3+} ($1\% \le x \le 7\%$) samples are consistent with the data reported for $KSrPO_4$ in JCPDS file no. 33-1045. As for $KSr_{1-x}PO_4$:xTb^{3+} samples, further increase of Tb^{3+} concentration (more than 7 mol%) leads to traces of impure phase signed by symbol "*".

The photoluminescence excitation (PLE) spectra ($\lambda_{emission}$ = 544 nm) series of $KSr_{1-x}PO_4$:xTb^{3+} ($1\% \le x \le 7\%$) samples are essentially the same except the intensity. For representation, the PLE spectrum of $KSr_{0.95}PO_4$:5%Tb^{3+} in the range of 120–300 nm is presented in Fig. 2. It is observed that the PLE of $KSr_{0.95}PO_4$:5%Tb^{3+} exhibits a broad excitation band located at 141 nm and a shoulder peak at 157 nm in the region of 120–162 nm. Considering host absorption band is rarely affected by activators, the VUV excitation spectrum of $KSr_{0.995}PO_4$:0.5%Eu^{2+} ($\lambda_{emission}$ = 426 nm) measured under the same conditions was also

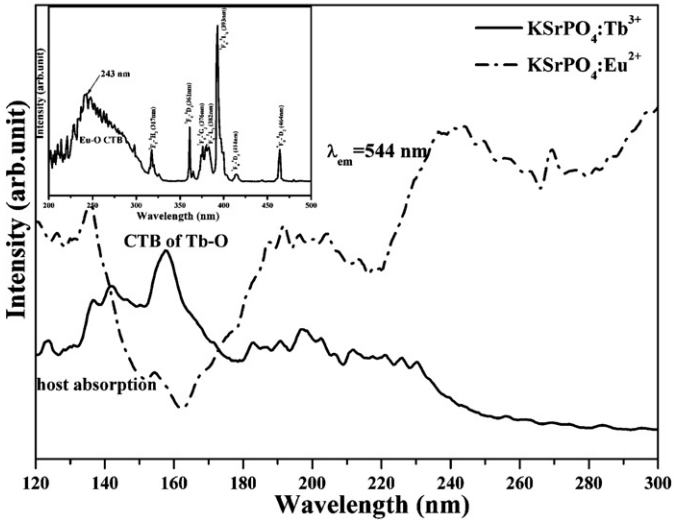

Fig. 2. Vacuum ultraviolet (VUV) excitation spectra of $KSr_{0.995}PO_4$:0.5%Eu^{2+} and $KSr_{0.95}PO_4$:5%Tb^{3+} monitoring at 426 nm and 544 nm at room temperature, respectively. The inset gives ultraviolet (UV) excitation spectrum ($\lambda_{emission}$ = 611 nm) of $KSr_{0.98}PO_4$:2%Eu^{3+} at room temperature.

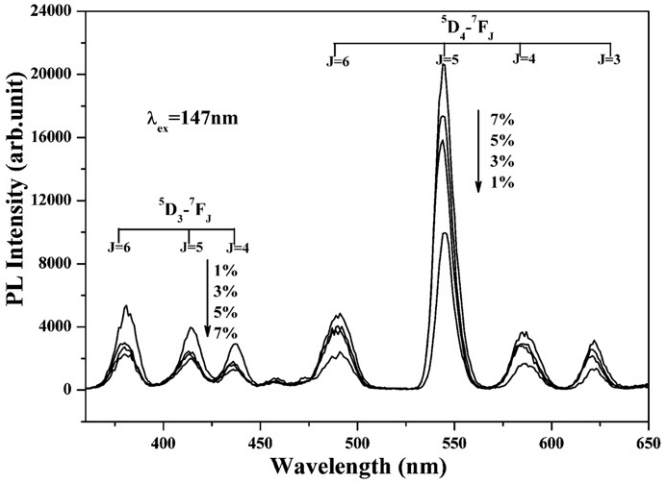

Fig. 3. Photoluminescence (PL) spectra ($\lambda_{excitation}$ = 147 nm) of $KSr_{1-x}PO_4$:xTb^{3+} ($1\% \le x \le 7\%$) at room temperature.

shown in Fig. 2 in order to investigate the attribution of these bands. Both the samples exhibit a broad band in the region of 120–162 nm. Thus, the band from 120 to 162 nm can be considered to include host absorption. In addition, it is found that the shoulder peak at 157 nm, which is overlapped with the host absorption, is only observed in the PLE spectrum of $KSr_{0.95}PO_4$:5%Tb^{3+}, therefore, it may be related to the absorption of $O^{2-} \rightarrow Tb^{3+}$. According to the formula (1) which is proposed by Resfeld and Jφrgensen [20], the position of the charge transfer band of the rare earths ions can be calculated.

$$E_{ct} \quad (\mathrm{cm}^{-1}) = [\chi opt(X) - \chi opt(M)] \times 30,000\,\mathrm{cm}^{-1} \qquad (1)$$

$\chi opt(X)$ and $\chi opt(M)$ are the optical electronegativities of the anion and central metal ion, respectively. The electronegativity of O^{2-} is variational in different hosts, and the $O^{2-} \rightarrow Eu^{3+}$ CT band could be observed easily in the UV region. Thus, the positions of other CT bands can be estimated after knowing the position of $O^{2-} \rightarrow Eu^{3+}$ CT band. The UV excitation spectrum of $KSrPO_4$:Eu^{3+} is given as insert in Fig. 2. As can be seen from it, the position of $O^{2-} \rightarrow Eu^{3+}$ CT band situates around 243 nm, viz. 41,152 cm^{-1}. Using the value of E_{ct} and χopt(Eu) which is reported to be 1.74 [21], the calculated electronegativity of O^{2-} is 3.11. Putting χopt(O) = 3.11 and χopt(Tb) = 0.95 [21] into Eq. (1), the CT band of $O^{2-} \rightarrow Tb^{3+}$ can be calculated to be 154 nm. Combining the PL spectra in Fig. 2 and the calculated result, the shoulder peak at 157 nm could be assigned to $O^{2-} \rightarrow Tb^{3+}$ absorption transition. From the analysis discussed above, the band spanning from 120 to 162 nm can be related to the host absorption transition and $O^{2-} \rightarrow Tb^{3+}$ CT band. The bands which cover the spectral range from 162 to 300 nm in the PLE spectrum of $KSr_{0.95}PO_4$:5%Tb^{3+} are due to transitions from the $4f^8$ single configuration to the energy levels $4f^75d^1$ mixed configuration of Tb^{3+}, and the crystal field splitting of d-levels of Tb^{3+} is reflected in this region. The PL spectra of $KSr_{1-x}PO_4$: xTb^{3+} ($1\% \le x \le 7\%$) samples under 147 nm excitation were presented in Fig. 3. As seen from Fig. 3, the characteristic transitions of Tb^{3+} ions strongly depend on the Tb^{3+} concentration. At lower Tb^{3+} concentration, the PL spectrum of Tb^{3+} is composed of two groups: the blue emissions below 450 nm are from $^5D_3 \rightarrow {}^7F_j$ (j = 4, 5, 6) transitions while the green and red emissions above 450 nm are from $^5D_4 \rightarrow {}^7F_j$ (j = 3, 4, 5, 6) transitions with the most intense emission at 544 nm corresponding to the $^5D_4 \rightarrow {}^7F_5$ transition of Tb^{3+}. Then, the $^5D_3 \rightarrow {}^7F_j$ (j = 4, 5, 6) transitions decrease gradually while the $^5D_4 \rightarrow {}^7F_j$ (j = 3, 4, 5, 6) transitions increase with increasing of Tb^{3+} concentra-

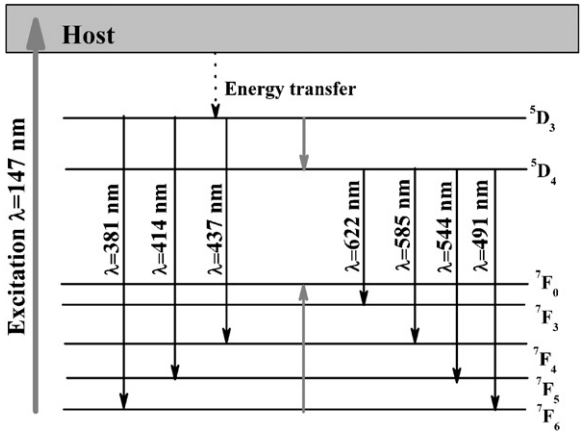

Fig. 4. A possible schematic diagram illustrating the cross relaxation process and emission process of Tb^{3+} in $KSrPO_4$ host.

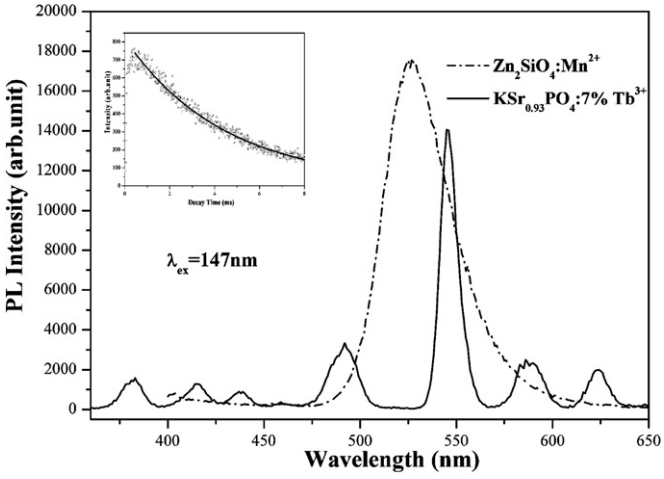

Fig. 5. Photoluminescence (PL) spectra ($\lambda_{excitation}$ = 147 nm) of $KSr_{0.93}PO_4$:7%Tb^{3+} and commercial Zn_2SiO_4:Mn^{2+} green phosphors at room temperature. The inset exhibits the decay curve ($\lambda_{excitation}$ = 147 nm) of the $^5D_4 \rightarrow {}^7F_5$ transition of Tb^{3+} in $KSr_{0.93}PO_4$:7%Tb^{3+}.

tion. This phenomenon is accordance with the results reported for $CaLnAl_3O_7$:Tb^{3+} (Ln = La, Gd) phosphors [22], and the reason can be considered to be cross-relaxation which can be expressed by the following process

$$Tb^{3+}(^5D_3) + Tb^{3+}(^7F_6) \rightarrow Tb^{3+}(^5D_4) + Tb^{3+}(^7F_0)$$

A possible schematic diagram illustrating the cross relaxation process and characteristic emission of Tb^{3+} in $KSrPO_4$ host is shown in Fig. 4.

Fig. 5 exhibits the comparison of the PL spectra between $KSr_{0.93}PO_4$:7% Tb^{3+} and the commercial Zn_2SiO_4:Mn^{2+} green phosphors by 147 nm excitation. The integrated intensity of $KSr_{0.93}PO_4$:7%Tb^{3+} is about 42% of the commercial Zn_2SiO_4:Mn^{2+} green phosphors, and the color coordinates were calculated to be ($x = 0.317$, $y = 0.522$) for $KSr_{0.93}PO_4$:7%Tb^{3+} sample. The inset shows the decay curve of Tb^{3+} $^5D_4 \rightarrow {}^7F_5$ transition in $KSr_{0.93}PO_4$:7%Tb^{3+}. The decay curve has been analyzed by curve fitting and it is found that the decay curve can be fitted perfectly using the single- order exponential decay function

$$I = A \exp\left(\frac{-t}{\tau}\right) \quad (2)$$

where I is the phosphorescence intensity at time t, A is a constant, and τ is the decay time for exponential component. The decay time extracted from the fitted curve is about 4.37 ms.

4. Conclusion

The green-emitting phosphors $KSr_{1-x}PO_4$:xTb^{3+} ($1\% \le x \le 7\%$) were successfully prepared via a solid-state process. Monitoring at 544 nm of the Tb^{3+} $^5D_4 \rightarrow {}^7F_5$ transition, the PLE spectrum in VUV region showed a band below 162 nm and a shoulder peak at 157 nm, which can be considered to be host absorption and charge transfer transition of $O^{2-} \rightarrow Tb^{3+}$, respectively. The PL investigation showed the optimal concentration of Tb^{3+} is about 7 mol% in $KSrPO_4$ host. The integrated intensity of the optimum compound $KSr_{0.93}PO_4$:7%Tb^{3+} is as much as 42% of commercial Zn_2SiO_4:Mn^{2+} and the decay time is about 4.37 ms. In view of further foundation work, the investigation of photoluminescence properties of $KSrPO_4$:Tb^{3+} in VUV region provides a few of experiment data and would be helpful for exploring VUV mechanism.

Acknowledgments

This work was supported by the National Natural Science Foundation of China (NSFC No. 10874061), Doctoral Program Foundation of Institutions of Higher Education of China (Grant No. 20040730019) and the Project of the Combination of Industry and Research by the Ministry of Education and Guangdong Province of China (Grant No. 0712226100023).

References

[1] Z.J. Zhang, J.L. Yuan, C.J. Duan, D.B. Xiong, H.H. Chen, J.T. Zhao, G.B. Zhang, C.S. Shi, J. Appl. Phys. 102 (2007) 093514.
[2] Y. Wang, H. Gao, Electrochem. Solid State Lett. 9 (2006) H19.
[3] C. Okazaki, M. Shiiki, T. Suzuki, K. Suzuki, J. Lumin. 87–89 (2000) 1280.
[4] Z. Zhang, Y. Wang, J. Zhang, Mater. Lett. 62 (2008) 846.
[5] A.W. de Jager-Veenis, A. Bril, J. Electrochem. Soc. 123 (1976) 1253.
[6] C.R. Ronda, J. Lumin. 72–74 (1997) 49.
[7] J. Koike, T. Kojima, R. Toyonaga, A. Kagami, T. Hase, S. Inaho, J. Electrochem. Soc. 126 (1979) 1008.
[8] C.H. Kim, I.E. Kwon, C.H. Park, Y.J. Hwang, H.S. Bae, B.Y. Yu, C.H. Pyun, G.Y. Hong, J. Alloys Compd. 311 (2000) 33.
[9] C.R. Ronda, J. Alloys Compd. 225 (1995) 534.
[10] T. Jüstel, J.C. Krupa, D.U. Wiechert, J. Lumin. 93 (2001) 179.
[11] K. Kim, Y.M. Moon, S. Choi, H.K. Jung, S. Nahm, Mater. Lett. 62 (2008) 3925.
[12] L. Tian, B.Y. Yu, C.H. Pyun, H.L. Park, S. Mho, Solid State Commun. 129 (2004) 43.
[13] L.Y. Zhou, F.Z. Gong, J.X. Shi, M.L. Gong, H.B. Liang, Mater. Res. Bull. 43 (2008) 2295.
[14] L. Zhou, W.C.H. Choy, J. Shi, M. Gong, H. Liang, T.I. Yuk, J. Solid state Chem. 178 (2005) 3004.
[15] X. Wu, H. You, H. Cui, X. Zeng, G. Hong, C.H. Kim, C.H. Pyun, B.Y. Yu, C.H. Park, Mater. Res. Bull. 37 (2002) 1531.
[16] L. El Ammari, M. El Koumiri, W. Depmeier, K.F. Hesse, B. Elouadi, Eur. J. Solid State Inorg. Chem. 34 (1997) 563.
[17] C.C. Lin, R.S. Liu, Y.S. Tang, S.F. Hu, J. Electrochem. Soc. 155 (2008) J248.
[18] Y.S. Tang, S.F. Hu, C.C. Lin, N.C. Bagkar, R.S. Liu, Appl. Phys. Lett. 90 (2007) 151108.
[19] Y. Huang, W. Kai, Y. Cao, K. Jang, H.S. Lee, I. Kim, E. Cho, J. Appl. Phys. 103 (2008) 053501.
[20] R. Resfeld, C.K. Jφrgensen, Lasers and Excite States of Rare Earth, Springer-Verlag, Berlin, 1977, p. 45.
[21] Q. Su, in: Proceedings of the Second Conference on Rare Earth Development and Application, J. Rare Earths (Special Issue) 2 (1991) 765.
[22] Y.H. Wang, D.Y. Wang, J. Electrochem. Soc. 153 (2006) H166.